An assessment of static and dynamic models to predict water treatment works performance

Roger Swan, John Bridgeman and Mark Sterling

ABSTRACT

The relative accuracy of static and dynamic water treatment works (WTWs) models was examined. Case study data from an operational works were used to calibrate and verify these models. It was found that dynamic clarification, filtration and disinfection models were more accurate than static models at predicting the final water quality of an operational site but that the root mean square errors of the models were within 5% of each other for key performance criteria. A range of abstraction rates at which the WTWs was predicted to operate adequately were identified using both types of models for varying raw water qualities. Static clarification, filtration and disinfection models were identified as being more suitable for whole works optimisation than dynamic models based on their relative accuracy, simplicity and computational demands.

Key words | accuracy, dynamic, model, Monte-Carlo, static, water treatment works

Roger Swan (corresponding author)
Mouchel Consulting,
Kier, 2 Parade,
Sutton Coldfield B72 1PH,
UK
E-mail: *roger.swan@mouchel.com*

John Bridgeman
Mark Sterling
School of Civil Engineering,
University of Birmingham,
Edgbaston B15 2TT,
UK

INTRODUCTION

Numerical modelling of water treatment works (WTWs) offers a means by which designers and operators can assess the likely impact of changes to raw water quality or process modifications on treated water quality. These assessments can be carried out with no risk posed to operational performance or consumer health and usually at lower cost than alternative pilot plant studies. The production of these models can result in a greater understanding of the treatment processes' mechanisms and the models themselves can be used for optimisation (van Leeuwen *et al.* 2005; Rietveld *et al.* 2010) and training purposes (Rietveld *et al.* 2004; Worm *et al.* 2010).

Due to the complex, multiple, non-linear relationships between raw water quality, WTW design, operating regime, final water quality and operating costs, the prediction of acceptable WTW performance is challenging. Existing water treatment modelling programs, such as OTTER (WRc), Stimela (Delft University of Technology) and Metrex (Duisberg University of Technology) have been found to be capable of modelling whole works comprehensively and have been successful when used in previous

studies (Rietveld & Dudley 2006; Dudley *et al.* 2008). The accuracy of these models, although sufficient to offer interesting insights into potentially effective treatment options and rough design parameters, has not historically been sufficiently accurate to replace laboratory or pilot plant testing for operational purposes (Dharmappa *et al.* 1994; Gupta & Shrivastava 2006). Models used in previous studies have also required relatively extensive calibration data (Rietveld & Dudley 2006; Dudley *et al.* 2008) and have only had their accuracy assessed over limited periods, usually less than 1 month (Adin & Rebhun 1977; Saatci & Oulman 1980; Edzwald *et al.* 1992; Head *et al.* 1997).

Water treatment models previously developed are based on a mixture of fundamental scientific principles and empirical relationships with the processes simulated using either static or more computationally demanding dynamic methods. This paper compares the accuracy of static and dynamic clarification, filtration and disinfection models to predict the performance of an operational WTW over multiple seasons, using data historically recorded for quality control purposes. The models were also used to predict
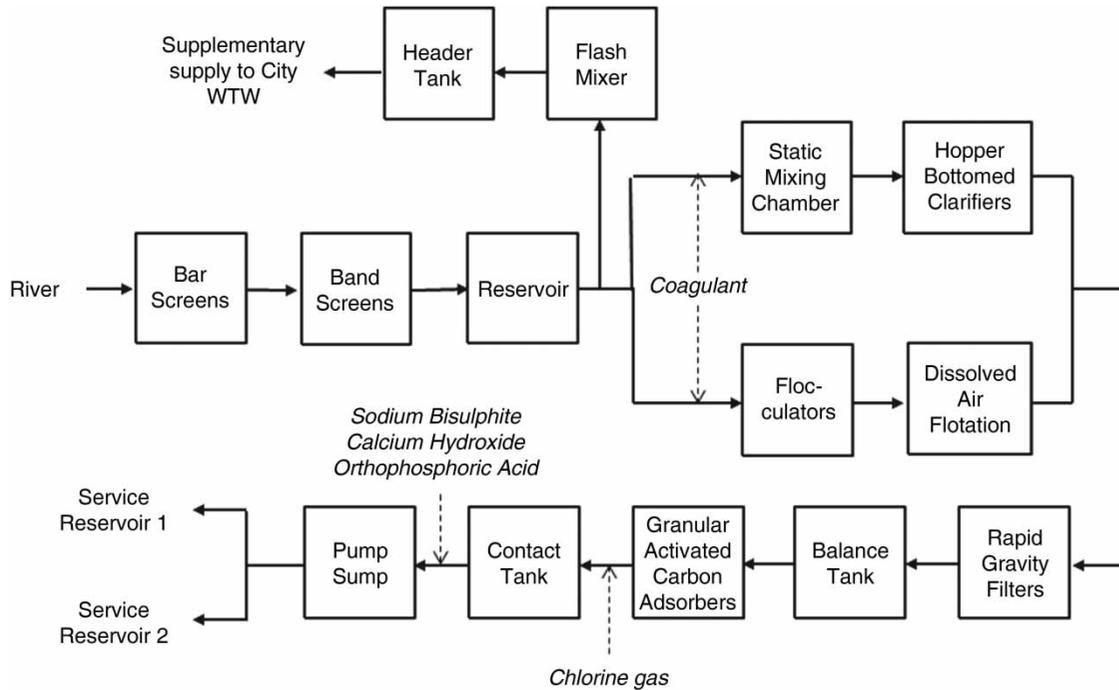
Figure 1 │ WTW schematic.

under what conditions an operational works was expected to produce water of an acceptable quality. This method provides simple guidance from a WTW model that can be applied by operational staff in real time.

METHODS

Site description

The WTW from which case study data were used (see Figure 1) is based in a rural location with water abstracted from a lowland reach of a river which is impounded in a reservoir prior to treatment. An overview of the reservoir water quality and chemicals dosed in 2011 is provided in Table 1. The water treated is divided into two treatment streams, one of which has hopper bottomed clarifiers (HBCs) and the other dissolved air flotation (DAF) to effect clarification. In both streams, ferric sulphate is dosed as coagulant before flocculation and clarification take place. Post-clarification, the waters are blended before being filtered through dual media (anthracite/sand) rapid gravity filters (RGFs). The water then passes through a

Table 1 │ Raw water quality and chemical dosing conditions observed 2011

Parameter	Mean	Standard deviation
Alkalinity (mg $CaCO_3$/L)	78	28
Bromide (µg/L)	63	12
Turbidity (NTU)	4.7	7.5
TOC (mg/L)	4.7	0.8
Temperature (°C)	12	5
Ultraviolet absorption (cm^{-1})	0.18	0.05
pH	7.7	0.4
Ferric sulphate dosed to DAF stream (mg as Fe^{3+}/L)	16	2
Ferric sulphate dosed to HBC stream (mg as Fe^{3+}/L)	14	2
Contact tank inlet free chlorine concentration (mg/L)	1.6	0.1

balance tank, to reduce the fluctuations in discharge that are caused by the backwashing of the filters, before being treated by granular activated carbon (GAC) adsorbers. Chlorine gas is dosed upstream of the contact tank controlled by a feedback loop linked to the free chlorine

concentration entering and exiting the contact tank. Sodium bisulphite is dosed to disinfected water to reduce the free chlorine to a residual concentration for distribution. Throughout the WTW, in-line sensors measure specific water quality parameters (WQPs) at 15-minute intervals. These data are transferred to an electronic supervisory control and data acquisition (eSCADA) system, stored on site, and archived off site. A maximum treatment capacity of 2,500 m³/h (60 ML/d) is achievable at the site. Further treatment process details are provided in Table 2.

Static and dynamic modelling approaches

Where the parameter values within a model have no dependency on past events, the model is described as static or steady state. An example of a steady state model is an algebraic equation where the current input values are all that is needed to calculate the output value, irrespective of any previous input or output values. Conversely, a dynamic model is time-dependent and previous parameter values of the model influence current values. The use of differential equations in a finite difference approach to model the accumulation of solids in filter layers is an example of a dynamic model. In this case, previous solids accumulation within the filter would reduce the solids removal efficiency of the filter. Other parameters which can only be modelled dynamically include the solids concentration of sludge blankets or chemicals in mixed containers where initial concentrations fluctuate. The benefits and limitations of both type of model are listed in Table 3.

Operational data

Fifteen-minute eSCADA and monthly water quality assurance test data from 2011 were used for calibration and data from the first 9 months of 2012 were used for verification. Data covering the whole of 2012 were not used as some of the required parameter data did not cover the entire period. The specifications of the sensors used is provided in Table 4 and a review of the accuracy of the manual measurements in comparison to Analytical Quality Control (AQC) samples is given in Table 5.

Table 2 | Treatment process details

Process	HBCs	DAF clarifiers	RGFs	Contact tanks
Number of units	Ten in continuous use	Seven available, brought into service as required	Eight in continuous use	Two in parallel
Dimensions	Surface length: 10 m; Surface width: 10.00 m; Depth top square section: 1.83 m; Depth hopper section: 7.62 m; Base length and width: 2.00 m; Volume: 498 m³	Width: 5.12 m; Initial depth: 1.65 m; End depth: 2.23 m; Contact zone length: 1.09 m; Contact zone volume: 9.2 m³; Separation zone length: 6.78 m; Total volume: 78 m³	Length: 13 m; Width: 4.5 m; Top anthracite depth: 0.60 m; Middle sand depth: 0.80 m; Base gravel depth: 0.40 m	Length: 32.18 m; Width: 7.5 m; Operational depth: 5 m; Total volume: 2,400 m³
Individual tank discharge	Discharge: 65 m³/h	Discharge: 240 m³/h	Discharge: 180 m³/h	Discharge: 635 m³/h
CT	CT: 7.5 h	CT: 20 min	Superficial velocity: 3 m/h	CT: 115 min
Chemical dose and other operational parameters	Ferric sulphate: 15 mg/L	Ferric sulphate: 17 mg/L; Air supply: 7 mg/L; Saturator pressure: 4 absolute bar; Recycle rate: 10%	Backwash duration: 48 hours; Head loss limit: 2 m; Turbidity limit: 0.5 NTU	Free chlorine dose: 1.6 mg/L; Residual chlorine: 1.3 mg/L; Number of baffles: 2

Table 3 │ Benefits and limitations of dynamic and static models

Characteristic	Dynamic	Static
Computational demand	Greater	Less
Suitability for modelling fluctuating conditions	Greater	Less
Sampling frequency of conditions required	Yes	No
Ease of application/understanding	Less	Greater

Table 4 │ Sensor specification

Parameter	Specification
Temperature (°C)	*YSI Sonde multi-head unit* Resolution 0.01°C Accuracy ±0.15°C
Discharge (ML/d)	*Siemens' Magflo 3000 electromagnetic flow meter* Accuracy ±0.25%
Turbidity (NTU)	Sigrist AquaScat WTM used throughout WTW except at filters and final waters where Hach 1720D is used *Hach 1720D* Accuracy ±2% or ±0.02 NTU (whichever greater) from 0 to 40 NTU *Sigrist AquaScat WTM turbidity meter* Resolution 0.001 FNU Accuracy not specified
Head loss (m)	*Endress + Hauser Deltabar PMD 130* Accuracy ±1%
Free chlorine (mg/L)	*Capital Controls Series 1930* Sensitivity 0.004 mg/L Display resolution 0.01 mg/L Accuracy ±0.1 mg/L

Process models

The models were programmed using Simulink, an extension of MATLAB that provides an interactive graphical environment for modelling time-varying systems. Process models were built as modules that could be grouped together to represent whole WTWs. The ODE45 solver was used with a variable time step for all of the models in this work with a minimum time step of 15 minutes, which is commonly the eSCADA data time step observed at the case study works. The mechanisms used to model the works both dynamically and statically are described below and an illustration of the model structure is shown in Figure 2.

The clarification (DAF and HBC), filtration and disinfection processes were all modelled statically and dynamically for comparative purposes. The coagulation and GAC processes, which were only modelled statically, were included so that the influence of varying organic matter concentrations on the solids removal and disinfection models could be assessed.

Degree of mixing

Continuous stirred tank reactors (CSTRs) were used to model the degree of mixing that occurs within processes in the dynamic models. A single CSTR models perfect mixing. The more tanks there are, the more the tanks act like a plug flow system. Ordinary differential Equations (1), (5) and (12) were used to model decay processes where mixing occurred. The static models assumed plug flow conditions and decay was represented using exponential decay Equations (2), (4) and (13).

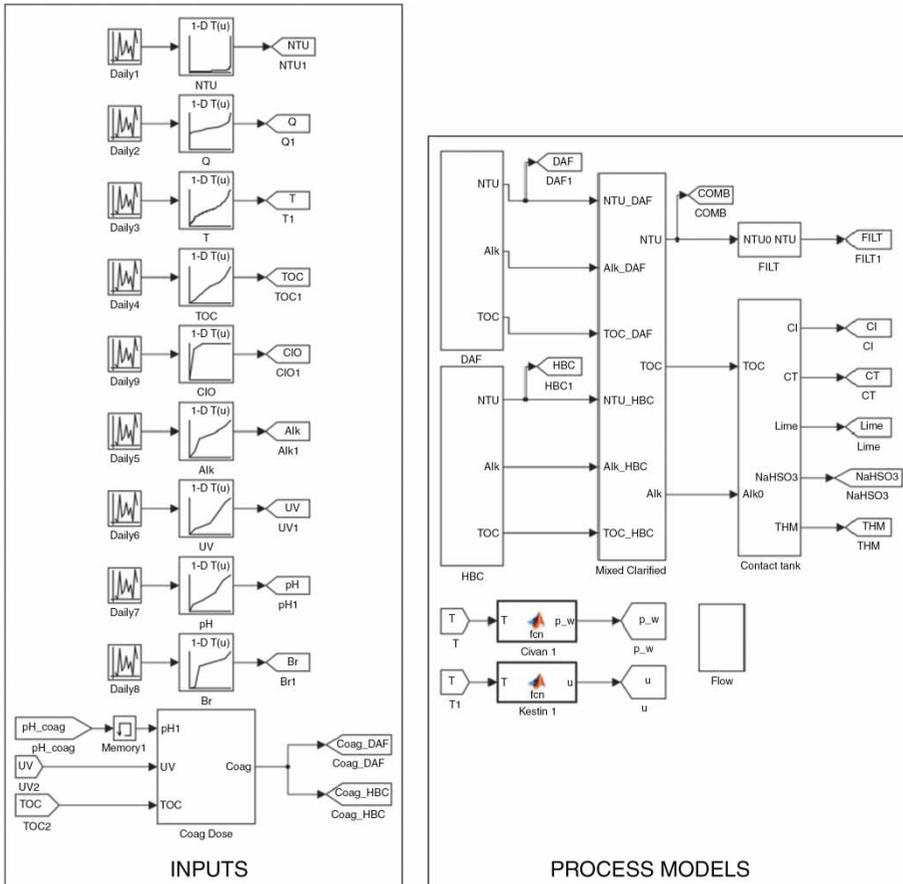## Correlation between suspended solids and turbidity

Many water treatment solids removal models use suspended solids (X_{TSS}) as a performance parameter. Most WTWs however, routinely measure turbidity as a surrogate parameter for X_{TSS} concentration. The ratio between suspended solids (mg/L X_{TSS}) and turbidity (*NTU*) was set at 2:1. This ratio was used as the default value in the OTTER program (WRc 2002) and is suggested by Binnie *et al.* (2006), where sufficient data are not available to define it more accurately. This ratio was used so the accuracy of WTW models which only use conventionally collected measurements could be assessed. This ratio may vary temporally and spatially in practice but is likely to range from 0.7 to 2.2 for low colour water that predominantly required turbidity removal treatment (AWWA 1999).

Coagulation by metal based coagulants

Assuming that all of the metal ions in the ferric or aluminium based coagulants form metal hydroxides, which precipitate out of solution, then by stoichiometric analysis, the amount of suspended solids (SS) added by ferric sulphate is 1.9 g/g Fe^{3+} and by alum 2.9 g/g Al^{3+}. Additional solids loading

Table 5 | Accuracy of manual measurements

Parameter	Basis of analytical procedure	Current bias from routine AQC (regulatory limit)	Current precision from routine AQC (regulatory limit)
Alkalinity as $CaCO_3$	Acid titration to end point of pH 4.5 using auto-titrator	−0.9% (5%)	2.4% (5%)
Bromide	Ion chromatography with conductimetric detection	0.3%	2.3%
pH	pH electrode	0.03 pH units (0.1 pH units)	−0.02 pH units (0.2 pH units)
Specific absorbance at 254 nm	UV spectrophotometry	−2.0%	4.0%
TOC	TOC analyser – UV/persulphate digestion of organic carbon and detection of released CO_2 by infra-red (NDIR)	−1.0% (5%)	2.0% (5%)
THM	Headspace GCMS (gas chromatography mass spectrometry). Total THM is the sum of four individual compounds: (a) chloroform (b) bromoform (c) bromodichloroform (d) dibromochloroform	(a) −2.3% (12.5%) (b) 1.1% (12.5%) (c) −5.0% (12.5%) (d) 2.7% (12.5%)	(a) 4.7% (12.5%) (b) 5.2% (12.5%) (c) 3.3% (12.5%) (d) 4.0% (12.5%)

Figure 2 | MATLAB/Simulink model.

caused by the precipitation of metal-natural organic matter (NOM) complexes or adsorption of total organic carbon (TOC) on to the surface of the metal hydroxides were not calculated. This was a limitation of the method.

The Edwards (1997) model, based on the Langmuir equation, was used to model dissolved organic carbon (DOC) removal due to coagulation. The extent of DOC removal is predicted by the raw water's DOC concentration, ultraviolet absorption at 254 nm and the coagulated water's pH. In the Edwards (1997) model, organic matter is assumed to be adsorbed onto the surface of metal hydroxide flocs that are formed by ferric or alum coagulants. The metal hydroxide ions Fe^{3+} and Al^{3+} are considered to be almost completely insoluble over the operational pH range and so the available sorbent surface is considered to be proportional to the dose of coagulant (Edwards 1997). Some of the organic matter is assumed to be non-adsorbable and the rest exists in equilibrium, between solution and adsorption, which is described by a Langmuir isotherm. The removal of DOC occurs during clarification but is considered to be dependent on the coagulation process. This assumes effective flocculation and clarification are occurring.

The 'general low DOC' parameters reported by Edwards (1997) are used to model TOC in this work. The application of these parameters for TOC application is considered to be appropriate as TOC typically approximates to DOC to within 2–17% for low turbidity water sources (Owen et al. 1995). The standard error of the model is estimated as being approximately ±20% or 0.5 mg/L (Swan 2015).

The influence of chemical addition on pH is calculated using the carbonate chemistry described in Stumm & Morgan (1970) and Snoeyink & Jenkins (1980) and is similar to the method described in Najm (2001), which was independently developed. The coagulation process is treated as a closed system and ionic strength effects are assumed to be negligible due to the low concentrations of chemicals found in water treatment. Instabilities in this carbonate model are limited through the application of the Newton–Raphson method to iteratively calculate pH.

Hopper bottomed clarification

In the dynamic model, the floc blanket clarifiers are modelled using a similar method to that presented in Head et al. (1997). The model's application differs from Head et al. (1997), firstly by not using works specific Barnea & Mizrahi (1973) equation parameters. Values from Head et al. (1997) were used to see how effectively modelling of a works could be achieved using only existing data collected from a WTW (shape factor s = 1, exponent factor n = 2.425, maximum settling velocity v_{max} = 5.65 m/h and minimum suspension concentration C_{min} = 10%). Secondly, the settlement of flocs was not modelled due to the relative dominance of blanket removal (approximately 1% of solids removed were found to be due to settlement under the conditions observed). Finally, two CSTRs were used rather than one, as this gave a more accurate replication of works performance (Swan 2015).

The Head et al. (1997) model was found to give good predictions of plant performance based on it predicting blanket concentration to ±5% and clarified turbidity to ±0.5 NTU. HBCs are represented by a series of homogeneous CSTR sections. Within a CSTR, solids either pass through or are absorbed into a sludge blanket. The model is based on the assumption that the flocs are bimodal, with smaller initial flocs and larger flocs within the blanket. All initial flocs are also assumed to be equally well removed by the sludge blanket. The SS removal within each CSTR of the dynamic model are calculated using Equation (1):

$$\frac{dX_{TSS}}{dt} = \frac{Q}{V}(X_{TSS_0} - X_{TSS}) - X_{TSS}(k_f \Phi H_b/L) \tag{1}$$

where Q = flow rate (m^3/h); V = volume CSTR = 249 m^3; X_{TSS_0} = flocculated suspended solids (mg/L); X_{TSS} = clarified suspended solids (mg/L); K_f = floc factor (h^{-1}); H_b = height of blanket (m); H_b/L = proportion of CSTR beneath blanket; Φ = mean blanket concentration (%V/V).

Making the assumptions that the blanket concentration and height remain consistent and the flow through the clarifier is plug flow, the removal of solids was modelled as an exponential decay equation in the static model:

$$X_{TSS} = X_{TSS_0} \times \exp^{-kt} \tag{2}$$

where t = contact time (h) and k = clarification efficiency parameter (h^{-1}).

DAF clarification

The attachment efficiency of bubbles onto SS by DAF was based on Equation (3) (Edzwald 2006). These are based on the plug flow assumption of flow through the contact zone which was found to be approximately true (Edzwald 2006). Removal is modelled in the static model using Equation (4) where attachment is assumed to occur only in the initial contact zone. In order to make the Edzwald model dynamic, mixing is applied through the use of a representative number of CSTRs and the entire tank is modelled as a contact zone. This is represented by Equation (5) as used in the OTTER program (WRc 2002). In this model, no flocculation occurs within the DAF tank and the removal performance is unaffected by the accumulation of floating sludge.

$$b = \frac{(3/2)\alpha\eta_T\phi_b v_b}{d_b} \tag{3}$$

$$X_{TSS} = X_{TSS_0} \times \exp^{-bt} \tag{4}$$

$$\frac{dX_{TSS}}{dt} = \frac{QX_{TSS_0}}{V} - \left(\frac{Q}{V} + b\right)X_{TSS} \tag{5}$$

where X_{TSS} = clarified suspended solids (mg/L), X_{TSS_0} = raw water suspended solids (mg/L), t = time (h), Q = flow-rate (m^3/h), V = volume of flotation tank = 78 m^3, b = floc flotation parameter (h^{-1}), α = attachment coefficient (dimensionless), η_T = individual bubble collision efficiency = 0.72, ϕ_b = bubble volume concentration (dimensionless), v_b = bubble rise rate (m/h), d_b = bubble diameter = 40 μm.

Rapid gravity filtration

The removal of solids by filtration was modelled using the Bohart & Adams (1920) model as shown in Equation (6), which is based on the following assumptions:

- the capacity of a media to remove substances reduces in proportion to the media capacity and the initial concentration of the substance being removed; and

- the rate of media capacity reduction is equal to the rate of substance removal.

$$\frac{X_{TSS}}{X_{TSS_0}} = \frac{1}{e^{\text{xka}_0/\text{v}-\text{tr}_t\text{SS}_0} + 1} \tag{6}$$

where X_{TSS_0} = flocculated SS (mg/L); X_{TSS} = clarified SS (mg/L); x = depth of filter media = 1.4 m; r_t = attachment coefficient at time t (h^{-1}); a_0 = filter capacity = 1,000 mg/L; v = superficial velocity of water through filter media (m/h) and t = time since last backwash (h).

As insufficient breakthrough was observed in the operational data, it was necessary to use a conservative estimate of the filter capacity (a_0) of 1,000 (mg/L). Filter ripening was modelled by adjusting the attachment coefficient (k) using an empirical relationship (Equation (7)). WRc (2002) found that this method gave a good fit to operational data. Through trial and error appropriate values were identified for the initial attachment factor and the ripening time to minimise root mean square error (RMSE) (Swan 2015).

$$r_t = r(1 - \alpha e^{-t/t_r}) \tag{7}$$

where r_t = attachment coefficient at time t; r = attachment coefficient; α = initial attachment factor = 1; t_r = ripening period = 1 h and t = time since last backwash (h).

The static model used the Bohart & Adams (1920) model as described above. In the dynamic model, the input SS concentration and the superficial velocity were taken as running means over a filtration run. This acted to dampen the response of the output turbidity to fluctuating water quality. Backwashes could also be triggered by head loss or filtered turbidity exceeding maximum limits in the dynamic model.

In the dynamic model, clean bed head loss was estimated on the assumption of Darcy flow (using the Kozeny–Carman Equation (8)) and head loss due to solids accumulation was calculated using Equation (9) (Adin & Rebhun 1977). The static model did not require head loss to be calculated as unscheduled backwashes were not modelled.

$$h_{L_0} = \frac{\kappa_k\mu[6(1-\varepsilon)/\psi d]^2 vL}{\rho_w g\varepsilon^3} \tag{8}$$

where h_{L_0} = clean bed head loss (m); K_k = Kozeny coefficient = 5; μ = water dynamic viscosity (Ns/m^2); ϵ = voidage = sand 0.4, anthracite 0.5; ψ = sphericity of filtration media = sand 0.8, anthracite 0.6; d = media diameter = sand 0.58 mm, anthracite 1.3 mm; v = filtration rate (m/h); L = filter bed depth = sand 0.8 m, anthracite 0.6 m and ρ_w = water density (kg/m^3).

$$h_L = \frac{h_{L_0}}{(1 - \beta \sqrt{\sigma})^3} \tag{9}$$

where h_L = head loss (m); σ = accumulated solids concentration (mg/L) and β = rate of head loss coefficient = 0.1 $\sqrt{l}/\sqrt{mg}$.

GAC

The GAC model predicted the removal of TOC, as a surrogate for natural organic matter. It was not possible to directly measure the influence of GAC on TOC removal at the examined WTW so TOC removal due to GAC adsorption and filtration was modelled as a reduction of 25%. This degree of removal was identified as suitable based on an assessment of Brown *et al.* (2011) data for six large WTWs, in the same region, for the summers of 2006 and 2007, with varying source waters and treatment processes.

SS removal by GAC was not be modelled, as although it has been shown to be at least as effective as conventional filtration media at removing SS from water (Love & Symons 1978), this is not the process's principal purpose at works where it is conventionally used as a tertiary treatment for removing a multitude of different dissolved organic compounds.

Chlorination

Flow within contact tanks resembles plug flow with a degree of dispersion. The flow regime of the contact tank is defined by the tanks hydraulic efficiency (t_{10}:t_θ). The hydraulic efficiency of a tank was defined as the ratio of the time taken for 10% of the concentration of a tracer chemical to be detected at the outlet of the tank (t_{10}) to the theoretical contact time (CT) if perfect plug flow conditions were present (t_θ).

A first order decay equation was used with decay constants based on values reported in Brown (2009) for six WTWs in the same region as the WTW examined in this work. The decay models used from Brown (2009) were for decay between 5 and 120 minutes (Equation (10) and Table 6). The initial decay was not modelled in this work as the initial chlorine recorded by the eSCADA system was at the inlet to the concentration tank after dosing occurred upstream:

$$K_b = A + (a \times S_{Cl_0}) + (b \times T) + (c \times Tot_{OC}) + (d \times S_{Br}) \tag{10}$$

where K_b = decay rate parameter (h^{-1}); S_{Cl_0} = chlorine dose = 1.6 mg/L; T = temperature ($^\circ$C); Tot_{OC} = total organic carbon (mg/L) and S_{Br} = Bromide (μg/L).

In the dynamic model, a representative number of CSTRs was identified by using an estimate of contact tank hydraulic efficiency (t10:tθ) using Equation (11) (Michalewicz 1996). A t10:tθ efficiency of 73% (as determined by a tracer test) resulted in 21 CSTRs being identified as being representative of the mixing that occurs. The decay within each CSTR was then calculated using Equation (12):

$$f = 1 - e^{-n(t/\bar{t})}\left[1 + n\frac{t}{\bar{t}} + \ldots + \left(n\frac{t}{\bar{t}}\right)^{n-1}\frac{1}{(n-1)!}\right] \tag{11}$$

where f = fraction of tracer that has passed through after time t; n = representative number of CSTRs; t = time since beginning of tracer test (min) and $\bar{t}$ = mean residence time (min).

$$\frac{dS_{Cl_{i+1}}}{dt} = \frac{Q \times (S_{Cl_i} - S_{Cl_{i+1}})}{V_{CSTR}} - K_b \times S_{Cl_{i+1}} \tag{12}$$

where $S_{Cl_{i+1}}$ = end free chlorine (mg/L), t = time (h), Q = contact tank discharge (m^3/h), S_{Cl_i} = start free chlorine (mg/L), V_{CSTR} = volume of CSTR = 114.3 m^3 and K_b = bulk chlorine decay parameter (h^{-1}).

Table 6 │ Mean parameters for initial 5-minute decay and bulk decay parameters, adapted from Brown (2009)

Relationship	A	a	b	c	d
$K_b \sim$ 5–120 mins	0.104	−0.134	0.0064	0.0504	0.00083

The decay within the static model was calculated using Equation (13):

$$S_{Cl} = S_{Cl_0} e^{-K_b t} \tag{13}$$

The formation of trihalomethanes (THMs) was modelled as being proportional to free chlorine consumption (Equation (14)) following Clark & Sivaganesan (1998), Hua (2000) and Brown *et al.* (2010). As the chlorine consumption was calculated using different methods, the predicted concentration of THMs was also model type dependent:

$$Tot_{THM} = K_{TC}(S_{Cl_0} - S_{Cl}) \tag{14}$$

where K_{TC} = coefficient of proportionality between Tot_{THM} and chlorine consumption = 45 μg/L per mg/L.

SS removal efficiency parameters

In order to improve the accuracy of the clarification and filtration models, a cross comparison of mean monthly reservoir WQPs (temperature, UV_{254}, TOC, specific UV absorbance (SUVA), turbidity, coagulant dose and estimated coagulated SS concentration) was made against monthly mean empirical removal efficiency parameters during 2011. Correlations were identified between raw turbidity and the removal efficiency parameters (two thirds of relationships had R^2 values greater than 0.5) and these relationships were used to estimate the removal parameters temporally.

The adjustment of the removal efficiency parameters indicates that the models were otherwise failing to replicate some mechanisms sufficiently to account for the higher removal rates observed for more turbid raw waters. The empirical removal parameters used are given in Table 7. The use of these relationships was found to reduce the RMSE of turbidity prediction for the static and dynamic model by between 16 and 74% for the calibration data. When applied to the verification data, RMSE was reduced by between 5 and 21% (Swan 2015).

Simulations

The performance of the works was simulated using time series input data described above and also coagulant doses

Table 7 │ Empirical removal parameters

Parameter	Empirical relationship	Applied to
Dynamic K_f (HBC)	$0.307*NTU_{Reservoir} + 3.689$ (for 2 CSTRs)	Equation (1)
Dynamic α (DAF)	$0.017*NTU_{Reservoir} + 2.05$ (for 1 CSTR)	Equation (4)
Dynamic r (FILT)	$0.0003*NTU_{Reservoir} + 0.0038$	Equation (7)
Static k (HBC)	$0.016*NTU_{Reservoir} + 0.494$	Equation (2)
Static α (DAF)	$0.007*NTU_{Reservoir} + 0.234$	Equation (4)
Static r (FILT)	$0.0005*NTU_{Reservoir} + 0.0034$	Equation (7)

from a predictive algorithm dependent on reservoir organics concentration and composition.

The predictive algorithm operated in the following way. Based on the reservoir TOC and ultraviolet adsorption at 254 nm (UV_{254}), the fraction of non-sorbable TOC was calculated using the Edwards (1997) model. This was then combined with a representative target clarified TOC concentration to calculate a target equilibrium concentration of adsorbate in solution (Ceq) using Equation (15):

$$C_{eq} = TOC_{target} - TOC_{non} \tag{15}$$

The coagulant dose was then calculated using Equation (16) derived from Edwards (1997):

$$M = \frac{(1 + bC_{eq})(TOC_0 - TOC_{non} - C_{eq})}{abC_{eq}} \tag{16}$$

where C_{eq} = equilibrium concentration of adsorbate in solution (mg/L); TOC_{target} = target TOC = 2.5 mg/L; TOC_{non} = non-sorbable TOC (mg/L); M = dose of coagulant (mMol Me^{3+}); b = Langmuir adsorption equilibrium parameter = 0.107 L/mg adsorbate; TOC_0 = initial TOC (mg/L); a = maximum adsorbent-phase concentration of adsorbate at saturation (mg/L adsorbate/mMol/L adsorbent).

The coagulant doses observed and predicted using the dosing algorithm can be seen in Figure 3. Only a single predicted coagulant dose was predicted for both clarification processes as an 'enhanced coagulation' dose should not be clarification process dependent. The RMSE between the predicted dose and that applied to the DAF process was ±3.5 mg Fe/L.
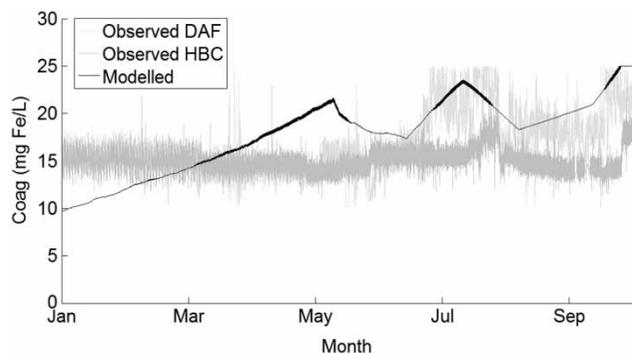
Figure 3 | Observed and modelled coagulant doses 2012.

In order that the performance of the WTW could be assessed for conditions other than those observed, synthetic time series data were produced using a Monte-Carlo approach. In the Monte-Carlo simulations, the model inputs were varied each simulated day for a simulated year, using randomly produced values from representative probability distributions.

Assessment

The accuracy of the models was assessed through an assessment of how closely the clarified and filtered turbidity, product of disinfection concentration and CT and THM production were replicated. This assessment was achieved using RMSEs, mean values and how often the key performance parameters failed to achieve target values representing 'good' performance for the WTW (as shown in Table 8). The 'failure' assessment gave an indication of how effective the model was at identifying the likelihood of unacceptable WTW performance for a given set of conditions.

A final set of simulations was carried out to identify an 'operating zone' for which the WTW was expected to

Table 8 | 'Good' operating performance criteria

Failure parameter	Failure condition
Blended clarified turbidity	>1 NTU
Filtered turbidity	>0.1 NTU
CT	<60 mg min/L
THM	>25 µg/L

produce water of an acceptable water quality. In defining the operating zone for the WTW, temperature and TOC concentration were selected as variable parameters alongside abstractions rate, due to their influence on both the solids removal and disinfection processes. Other water quality, design and operational parameters were assigned set values approximately equivalent to those observed in 2011. The values applied are given in Table 9. The coagulant dosing algorithm was applied.

The models were simulated for every combination of reservoir TOC concentration, temperature and abstraction rate listed in Table 9 (7,750 combinations) and operating zones were identified. Surface plots were then produced of the minimum and maximum abstraction rates which achieved the 'good' performance criteria.

Table 9 | Operating zone parameters used

Parameter	Value
HBC units	10
DAF units	7
RGF units	8
Contact tank volume	2,400 m^3
Filtration run length	48 hours
Proportion of abstracted water treated by DAF	0.55
DAF compressor pressure	400 kPa
Contact tank inlet free Cl concentration	1.6 mg/L (1.56 mg/L observed)
Reservoir turbidity	5 NTU (4.7 NTU observed)
Reservoir alkalinity	80 mg/L as CaCO3 (78 mg/L observed)
Reservoir UV254	0.17 cm^{-1} (0.173 cm^{-1} observed)
Reservoir pH	7.7 (7.72 observed)
Reservoir bromide	50 (63 µg/L observed)
Reservoir TOC concentration	1–10 mg/L in single unit increments (3.3–6.2 mg/L observed)
Reservoir temperature	0–30°C in single unit increments
Abstraction rate	100–2,500 m^3/h in 100 m^3/h increments
Clarified TOC target	2.5 mg/L
Time simulated	50 hours spin up, 50 hours measured

RESULTS AND DISCUSSION

The ability of the dynamic and static models to replicate the performance of the examined WTW in 2012 using time-series and Monte-Carlo conditions is shown in Tables 10 and 11. Figure 4 shows the operating zones identified.

The dynamic clarification, filtration and disinfection models were found to be more accurate than the static models at replicating key performance parameters (clarified and filtered turbidity, CT and THM production) under time-series conditions with observed coagulant doses being applied. The RMSE of the dynamic model was at least 5% less than that of the static model for the solids removal processes (HBC and DAF clarified

and RGF turbidity) and 1–3% less for the disinfection models (residual chlorine concentration, CT and THM formation) (see Tables 10 and 11).

It was necessary to predict coagulant dose as operators varied it substantially over the year based on observed clarified turbidity (dependent on floc formation) and judgement. As floc formation was not modelled and operator judgement was prohibitively complex to replicate, coagulant dose prediction allowed future or stochastic conditions to be modelled representatively. The coagulant dosing algorithm was found to show correlation with operator specified doses (see Figure 3). This suggests that TOC concentrations could be used to specify coagulant doses using a method derived from the Edwards (1997) TOC adsorption isotherm. If this type of coagulant dosing was applied at the

Table 10 │ Dynamic model accuracy

Parameter			DAF (NTU)	HBC (NTU)	FILT (NTU)	CT[a] (mg min/L)	THM (μg/L)
2012 observed		$\bar{x}$	0.68	0.44	0.079	109	9.9
		Failure	6.8%	0.1%	30.7%	0.1%	0.0%
Time series simulations	Simulated using observed coagulant dose	RMSE	0.28	0.18	0.035	24	3.0
		$\bar{x}$	0.63	0.45	0.077	114	7.8
		$\bar{x}$ absolute error	− 0.05	0.01	− 0.002	5	− 2.1
		Failure	0.2%	0.1%	18.1%	0.2%	0.0%
		Failure absolute error	− 6.6%	0.0%	− 12.6%	0.1%	0.0%
	Simulated using coagulant dose algorithm	RMSE	0.29	0.22	0.037	23	3.4
		$\bar{x}$	0.67	0.53	0.087	114	7.5
		$\bar{x}$ absolute error	− 0.01	0.09	0.008	5	− 2.4
		Failure	1.0%	2.4%	27.0%	0.2%	0.0%
		Failure absolute error	− 5.8%	2.3%	− 3.7%	0.1%	0.0%
Monte-Carlo simulations		$\bar{x}$ min	0.66	0.48	0.078	121	6.4
		$\bar{x}$ mean	0.66	0.48	0.079	121	6.7
		$\bar{x}$ max	0.66	0.49	0.081	122	7.1
		$\bar{x}$ absolute error	− 0.02 to −0.02	0.04–0.05	− 0.001 to 0.002	12–13	− 3.5 to −2.8
		Failure min	0.3%	0.2%	10.2%	0.0%	0.0%
		Failure mean	1.0%	1.6%	13.6%	0.0%	0.0%
		Failure max	2.2%	2.3%	15.3%	0.0%	0.0%
		Failure absolute error	− 6.5 to −4.6%	0.1–2.2%	− 20.5 to −15.4%	− 0.1 to −0.1%	0.0–0.0%

[a]To prevent disproportionate skew, 0.2% of outliers were removed from the original observed data set as they were outside of three standard deviations of the mean value.

Table 11 | Static model accuracy

Parameter			DAF (NTU)	HBC (NTU)	FILT (NTU)	CT[a] (mg min/L)	THM (μg/L)
2012 observed		$\bar{x}$	0.68	0.44	0.079	109	9.9
		Failure	6.8%	0.1%	30.7%	0.1%	0.0%
Time series simulations	Simulated using observed coagulant dose	RMSE	0.34	0.26	0.045	25	3.4
		$\bar{x}$	0.62	0.33	0.065	113	7
		$\bar{x}$ absolute error	−0.06	−0.11	−0.014	4	−2.9
		Failure	5.0%	1.1%	14.2%	0.2%	0.0%
		Failure absolute error	−1.8%	1.0%	−16.5%	0.1%	0.0%
	Simulated using coagulant dose algorithm	RMSE	0.35	0.26	0.049	22	3.5
		$\bar{x}$	0.66	0.4	0.074	113	7.2
		$\bar{x}$ absolute error	−0.02	−0.04	−0.005	4	−2.7
		Failure	5.7%	4.0%	21.5%	0.0%	0.0%
		Failure absolute error	−1.1%	3.9%	−9.2%	−0.1%	0.0%
Monte-Carlo simulations		$\bar{x}$ min	0.68	0.33	0.064	121	5.9
		$\bar{x}$ mean	0.68	0.33	0.065	121	6.5
		$\bar{x}$ max	0.69	0.34	0.067	122	7.0
		$\bar{x}$ absolute error	0.00–0.01	−0.11 to −0.10	−0.015 to −0.012	12–13	−4.1 to −3.0
		Failure min	13.7%	0.8%	10.9%	0.0%	0.0%
		Failure mean	15.6%	1.7%	14.0%	0.0%	0.0%
		Failure max	18.7%	2.6%	15.9%	0.0%	0.0%
		Failure absolute error	6.9–11.9%	0.7–2.5%	−19.8 to −14.8%	−0.1 to −0.1%	0.0–0.0%

[a]To prevent disproportionate skew, 0.2% of outliers were removed from the original observed data set as they were outside of three standard deviations of the mean value.
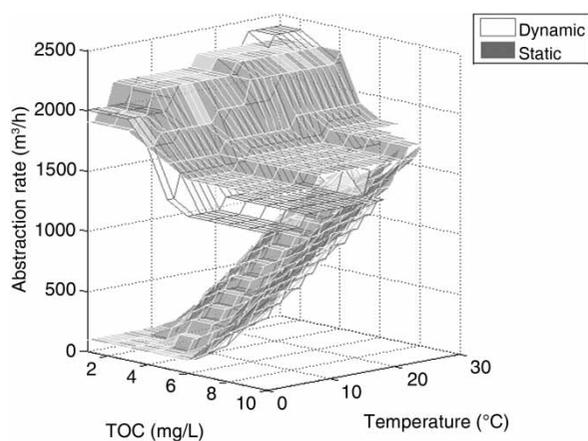
Figure 4 | Predicted operating zone.

investigated WTW, it is possible that coagulant could be dosed more efficiently. This could result in less variation in chlorine demand and THM production, due to a more stable pre-disinfection water organic content. The model predicted that the use of the dosing algorithm would also reduce coagulant costs by approximately £250,000 per year and sludge disposal costs by approximately £20,000 per year at the examined works.

The RMSE of the more computationally demanding dynamic clarification models were lower than the static models, but of a similar magnitude (RMSE ±0.1 NTU). A lower degree of accuracy is achieved in predicting DAF, in comparison to HBC clarified turbidity, using both types of models. The lower degree of accuracy is thought to be influenced by individual DAF tanks being brought in and out of service and tanks appearing to have substantially different removal efficiencies in practice. The influence of these effects needs to be considered when assessing the likelihood of unacceptable WTW performance for different treatment processes and operating regimes.

The dynamic filter model was found to be more accurate than the static model with RMSEs of 0.035 and 0.045 NTU respectively. Some of the additional error of the static

filtration model is due to unrepresentative turbidity fluctuation. This fluctuation is due to the static model not having a mechanism to dampen the influence of short term changes in operating conditions. The certainty in modelled filtered turbidity was limited, due to performance variation between filters in the same bank and difficulty in identifying robust process parameters such as attachment/detachment coefficients or filter capacities. Applying dynamic aspects to the static logistic curve approximation of filter performance improves predictive ability marginally. It is possible that a conservative estimation of filter performance could be achieved using the static Bohart & Adams (1920) equation with the time since last backwash parameter set as the filter run duration (in Equation (7)).

The dynamic model's RMSEs for predicting CT, THM formation and residual free chlorine concentration were found to be lower than those predicted using the static model, but of the same magnitude ($\pm3\%$). The accuracy of the models for predicting CT, THM formation and residual free chlorine concentration is approximately ±10, ±20 and $\pm30\%$, respectively.

When Monte-Carlo conditions were applied, the mean of the key performance parameters altered by up to 15% for the dynamic model and up to 20% for the static model, in comparison with the application of time series data (see Tables 10 and 11). This variation in performance is likely to be caused by the random nature of the Monte-Carlo process, inexact representation of operating conditions and lack of modelling of correlations between operating conditions (i.e. higher TOC concentrations may be expected when raw turbidity is greater) (Clark *et al.* 2011).

The range of mean key performance values, produced from three separate Monte-Carlo runs, was found to be less than 5%, with the exception of THM production. Application of the Monte-Carlo technique to assess the performance of WTWs has the potential to give insight into their robustness but with potentially reduced accuracy and precision.

The accuracy of the static and dynamic models to predict the likelihood that 'good' treatment could be achieved by the WTW under time-series and Monte-Carlo conditions was found to be comparable. The relative failure rates predicted by the static and dynamic models for the different performance parameters were found to be dependent on the treatment process modelled and the simulation method.

The percentage of the time that WTW key performance parameters failed their target values was found to be predicted with an accuracy of $\pm20\%$. The disinfection and disinfection by-product formation failure rates were predicted with the greatest accuracy ($\pm0.1\%$), followed by clarified turbidity ($\pm12\%$) and finally filtered turbidity. The failure rates predicted using Monte-Carlo methods had precisions of 6% for both models for all parameters and simulation methods.

The 'operating zone' identified using the dynamic and static models had similar minimum and maximum profiles (see Figure 4), indicating that the same causes of failure are likely to limit abstraction rates for both models. The models had comparable maximum abstraction rates for low initial TOC concentration conditions whilst the dynamic model had significantly lower maximum abstraction rates for higher initial TOC concentrations (>4 mg/L). The maximum abstraction rates predicted by the two models had disparities of up to $\pm25\%$ for similar conditions.

The models predict that as initial TOC concentration increases it is necessary to increase coagulant dose to limit the filtered residual TOC concentration (to reduce the impact on the adsorption and disinfection processes). The increased solids loading caused by metal hydroxides from coagulants being precipitated out of solution results in the maximum abstraction rate of the WTW reducing (due to elevated clarified or filtered turbidity at higher abstraction rates). It was predicted that minimum abstraction rates have greater influence at temperatures above 18°C and initial TOC concentrations above 6 mg/L. Under these conditions, the maximum and minimum abstraction rates were predicted to converge, making acceptable treatment unachievable for the defined treatment regime.

Although the models in the operational zone analysis predicted that warmer water would result in an increase in the maximum possible abstraction rate, global warming will not necessarily result in lower turbidity final waters. Climate change could influence other water properties such as alkalinity, hardness, TOC and ammonia concentrations. Clark *et al.* (2011) reported that for the Ohio River, TOC was predicted to increase in the future by 0.03 mg/L per annum. It is shown that controlling TOC concentrations using enhanced coagulation could reduce the maximum abstraction rate of a WTW considerably and so there is uncertainty as to the influence of climate change on the operation of WTWs.

As the data used to calibrate and verify the models came from an operational WTW, a limited range of performance was observed, due to the operators striving to provide a satisfactory water quality for consumers. When unsatisfactory performance was predicted, the model was likely to be operating at, or beyond, the range of the calibration and verification data, limiting confidence in the models' accuracies. However, the use of computational models can allow a wide range of treatment options to be initially assessed with no risk posed to operational performance or consumer health and at lower cost than alternative pilot plant studies.

CONCLUSIONS

The use of dynamic clarification, filtration and disinfection models using observed time-series initial conditions were found to be more accurate than static models. The RMSE of the dynamic model was at least 5% lower than the static model for clarified and filtered turbidity and 1–3% lower for CT disinfection and THM production (see Tables 10 and 11).

The application of Monte-Carlo conditions resulted in the predicted mean of key performance parameters (clarified and filtered turbidity, CT and THM production) adjusting by up to 15% for the dynamic model and up to 20% for the static model. The precision of these values over three runs was found to be less than ±5%.

The accuracy of the static and dynamic models to predict the likelihood that 'good' treatment (where the key performance parameters met set criteria) could be achieved by the WTW under time-series and Monte-Carlo conditions was found to be comparable.

The dynamic and static models identified similar 'operating zones' (see Figure 4). For temperatures above 18 °C and initial TOC concentrations above 6 mg/L, acceptable treatment was predicted not to be achievable for the required final water quality and defined treatment regime due to either insufficient solids removal or excessive THM production.

The justification for the complexity of the dynamic models assessed, along with the considerable amounts of calibration data they require, is limited for whole works modelling as their accuracies are comparable to their static alternatives. The application of static models

calibrated using process and telemetry data is considered to be more suitable for application to whole works modelling.

REFERENCES

Adin, A. & Rebhun, M. 1977 Model to predict concentration and head loss profiles in filtration. *J. Am. Water Works Assoc.* **69** (8), 444–453.

AWWA 1999 *Water Quality and Treatment: A Handbook of Community Water Supplies*, 5th edn. McGraw-Hill, New York.

Barnea, E. & Mizrahi, J. 1973 A generalized approach to the fluid dynamics of particulate systems: part 1. General correlation for fluidization and sedimentation in solid multiparticle systems. *Chem. Eng. J.* **5** (2), 171–189.

Binnie, C., Kimber, M. & Smethurst, G. 2006 *Basic Water Treatment*, 3rd edn. Royal Society of Chemistry, Cambridge.

Bohart, G. S. & Adams, E. Q. 1920 Some aspects of the behavior of charcoal with respect to chlorine. *J. Am. Chem. Soc.* **42**, 523–544.

Brown, D. 2009 *The Management of Trihalomethanes in Water Supply Systems*. PhD Thesis, University of Birmingham, UK.

Brown, D., West, J. R., Courtis, B. J. & Bridgeman, J. 2010 Modelling THMs in water treatment and distribution systems. *Proc. Inst. Civil Eng. Water Manage.* **163** (4), 165–174.

Brown, D., Bridgeman, J. & West, J. R. 2011 Understanding data requirements for trihalomethane formation modelling in water supply systems. *Urban Water J.* **8** (1), 41–56.

Clark, R. M. & Sivaganesan, M. 1998 Predicting chlorine residuals and formation of THMs in drinking water. *J. Environ. Eng.* **124** (12), 1203–1210.

Clark, R. M., Li, Z. W. & Buchberger, S. G. 2011 Adapting water treatment design and operations to the impacts of global climate change. *Front. Earth Sci.* **5** (4), 363–370.

Dharmappa, H. B., Vigneswaran, S., Verink, J. & Fujiwara, O. 1994 Water-treatment system-design for turbidity removal. *J. Environ. Eng. ASCE* **120** (4), 900–920.

Dudley, J., Dillon, G. & Rietveld, L. C. 2008 Water treatment simulators. *J. Water Supply Res. Technol. AQUA* **57** (1), 13–21.

Edwards, M. 1997 Predicting DOC removal during enhanced coagulation. *J. Am. Water Works Assoc.* **89** (5), 78–89.

Edzwald, J. K. 2006 Chapter 6: dissolved air flotation in drinking water treatment. In: *Interface Science in Drinking Water Treatment: Theory and Applications*, 1st edn (G. Newcombe & D. Dixon, eds). Academic Press, London, pp. 89–108.

Edzwald, J. K., Walsh, J. P., Kaminski, G. S. & Dunn, H. J. 1992 Flocculation and air requirements for dissolved air flotation. *J. Am. Water Works Assoc.* **84** (3), 92–100.

Gupta, A. K. & Shrivastava, R. K. 2006 Uncertainty analysis of conventional water treatment plant design for suspended solids removal. *J. Environ. Eng. ASCE* **132** (11), 1413–1421.

Head, R., Hart, J. & Graham, N. 1997 Simulating the effect of blanket characteristics on the floc blanket clarification process. In: *Proceedings of the 1996 IAWQ/IWSA Joint Group on Particle Separation, 4th International Conference on the Role of Particle Characteristics in Separation Processes*, 28–30 October, 1996. Jerusalem, Israel.

Hua, F. 2000 *The Effects of Water Treatment Works on Chlorine Decay and THM Formation*. PhD Thesis, University of Birmingham, UK.

Love, T. & Symons, M. 1978 *Operational Aspects of Granular Activated Carbon Adsorption Treatment*. US EPA. Available from: www.epa.gov/nscep (accessed 6 March 2012).

Michalewicz, Z. 1996 *Genetic Algorithms + Data Structures = Evolution Programs,* 3rd edn. Springer, Germany.

Najm, I. 2001 User-friendly carbonate chemistry charts. *J. Am. Water Works Assoc.* **93** (11), 86–93.

Owen, D. M., Amy, G. L., Chowdhury, Z. K., Paode, R., McCoy, G. & Viscosil, K. 1995 NOM – characterization and treatability. *J. Am. Water Works Assoc.* **87** (1), 46–63.

Rietveld, L. & Dudley, J. 2006 *D5.4.1 Models for Drinking Water: State of the Art*. Available from: www.techneau.org/fileadmin/files/Publications/Publications/Deliverables/D5.4.1.pdf (accessed 12 October 2010).

Rietveld, L. C., Van Schagen, K. & Van Dijk, J. C. 2004 Information technology for linking research to education and training in drinking water treatment. In: *Proceedings of the 2004 Water Institute of Southern Africa (WISA) Biennial Conference*. Cape Town, South Africa.

Rietveld, L. C., van der Helm, A. W. C., van Schagen, K. M. & van der Aa, L. T. J. 2010 Good modelling practice in drinking water treatment, applied to Weesperkarspel Plant of Waternet. *Environ. Model. Software* **25** (5), 661–669.

Saatci, A. M. & Oulman, C. S. 1980 The bed depth service time design method for deep bed filtration. *J. Am. Water Works Assoc.* **72** (9), 524–528.

Snoeyink, V. L. & Jenkins, D. 1980 *Water Chemistry*, 1st edn. Wiley, New York.

Stumm, W. & Morgan, J. J. 1970 *Aquatic Chemistry: An Introduction Emphasizing Chemical Equilibria in Natural Waters*, 1st edn. Wiley-Interscience, New York.

Swan, R. W. 2015 *Optimisation of Water Treatment Works Using Monte-Carlo Methods and Genetic Algorithms*. PhD Thesis, University of Birmingham, UK.

van Leeuwen, J., Daly, R. & Holmes, M. 2005 Modeling the treatment of drinking water to maximize dissolved organic matter removal and minimize disinfection by-product formation. *Desalination* **176** (1–3), 81–89.

Worm, G. I. M., van der Helm, A. W. C., Lapikas, T., van Schagen, K. M. & Rietveld, L. C. 2010 Integration of models, data management, interfaces and training support in a drinking water treatment plant simulator. *Environ. Model. Software* **25** (5), 677–683.

WRc 2002 *Otter Version 2.1.3 User Documentation*, 2nd edn. WRc, Swindon.